Ain Shams Engineering Journal (2015) 6, 947–956

Ain Shams University

Ain Shams Engineering Journal

www.elsevier.com/locate/asej
www.sciencedirect.com

MECHANICAL ENGINEERING

Transient analysis and improvement of indoor thermal comfort for an air-conditioned room with thermal insulations

D. Prakash *

School of Mechanical Engineering, SASTRA University, Thanjavur, Tamil Nadu, India

Received 24 September 2014; revised 25 December 2014; accepted 15 January 2015
Available online 6 March 2015

KEYWORDS

Thermal comfort;
Building insulation;
Predicted mean vote;
Computational fluid dynamics;
Air conditioned room

Abstract Thermal insulations over the building envelop reduce the heat gain due to solar radiation and may enhance good and uniform indoor thermal comfort for the occupants. In this paper, the insulation layer-wood wool is laid over the roof and exposed wall of an air-conditioned room and its performance on indoor thermal comfort is studied by computational fluid dynamics (CFD) technique. From this study, 3% of indoor thermal comfort index-predicted mean vote (PMV) is improved by providing wood wool layer. In addition, the optimum supply air temperature of air-conditioning unit for good thermal comfort is predicted as in the range of 299–300 K (26–27 °C).

1. Introduction

In buildings, thermal comfort is a vital factor that decides the occupant's health and productivity. Since 90% of the people spend most of their time inside the building, they are interested to invest high cost to live in a comfort environment with air conditioners and air coolers. Also the buildings in cities consume a large proportion of electrical energy mainly for HVAC (heating, ventilation, and air-conditioning) systems [1]. Even though the air conditioning unit controls the indoor temperature and provides good indoor comfort, occupants are still suffering from many health related symptoms like nose irritation, stuffed nose, rainy nose, eye irritation, cough, tightness in chest, fatigue, headache, rash and many more [2]. Hence it is very imperative to operate the air conditioning unit for reduced health related problems under less consumption of energy without sacrificing the thermal comfort. This can be achieved by operating the air conditioning unit at sufficient temperature level of air supply. Also the indoor thermal comfort should be maintained with a same value for a complete 24 h irrespective to the variations in solar radiation.

Among the many sources that gain the heat into the building, solar radiation is identified as the major factor that raises the indoor temperature. The incoming solar energy is absorbed by the earth surface as 51% and gets reflected by 4%; atmosphere and clouds absorb 19% and reflect 26% respectively. Vijayakumar et al. [3] stated that the heat transmission across the building roof is about 50–70% of the total heat entry of the

* Tel.: +91 9489036775.
E-mail address: prakash@mech.sastra.edu.
Peer review under responsibility of Ain Shams University.

Production and hosting by Elsevier

http://dx.doi.org/10.1016/j.asej.2015.01.005

room. Chou et al. [4] also stated that the heat gain through the roof due to solar radiation incident on the roof reaches more than 1000 W/m^2 in clear sky condition. Hence a good thermal insulation is required for both roof and exposed wall of an air conditioned and non air conditioned building to reduce the heat gain of the indoor. The thermal insulations in roof and exposed walls also reduce the capacity of air-conditioning system and the annual energy cost for a building. Also, it extends the periods of thermal comfort without reliance on air-conditioning unit especially during inter-season periods. In this contest, much research work has been made to reduce the heat transmission across the roof by adding insulation layers like phase change material, reflective coating, green roofs and etc. [5]. Barrios et al. [6] studied the effect of mono layered and multi layered roof/wall configuration in an air conditioned room and identified that providing such a insulation layer on the exterior side of the roof/wall gives a better thermal performance than placing the insulation layer on the interior sided of the wall/roof [7–9]. The thermal conductance coefficients (U-factor) of the non-insulated roof ranges from 7.76 (250 mm concrete) to 18.18 W/m^2 K (100 mm concrete) [10]. Therefore, the heat transfer across non-insulated roofs is greater than roofs with insulation. Al-Sanea and Zedan [11] studied the effect of insulation layer location on the heat transfer characteristics of building walls under steady periodic conditions. Halwatura and Jayasinghe [12] studied the impact of insulation (polyethylene) thickness and concluded that adding a 2.5-cm thick polyethylene insulation on the scaled concrete roof reduces the peak roof soffit temperature from 42 to 33 °C in the tropical climate of Sri Lanka. Alvarado et al. [13] studied the thermal performance of concrete-based roof prototypes with different types of insulations and found that the combined application of aluminum reflector and polyurethane insulation offers a heat flux reduction of 88% in comparison with the un-insulated roof prototypes. Ashok kumar and Suman [14] experimentally evaluated the impact of insulation material for walls and roof on indoor thermal comfort under composite climate. Hence, this study also interested to reduce the heat gain due to solar radiation by providing insulation layer over roof and wall of an air conditioned room through the analysis of indoor air flow characteristics.

The indoor air flow characteristics are studied either by small-scale or full-scale models. Small-scale models are constrained by the need of scaling factors for heat transfer and air flow, while the full-scale environmental chambers for indoor evaluations are expensive and practical experiments are time consuming. Nevertheless, computational fluid dynamics (CFD) technique plays an important role in the design and evaluation of indoor air flow characteristics, thermal comfort conditions, smoke conditions or air quality in worldwide large space buildings such as Yoyogi National Stadium in Japan [15], Galatsi Arena in Greece [16], Kansai Airport in Japan [17], Great Hall of the People in China [18], etc. Thus, in this study the CFD tool is employed to analyze the indoor thermal comfort of an insulated air conditioned room under various operating conditions of air conditioning unit.

2. Room model and CFD methodology

An isolated room of size width = 5 m and height = 4 m is considered in this study. This traditional room is having a roof thick of 0.15 m of concrete, 0.02 m thickness of weathering tile and 0.2 m of wall thickness. Later the traditional room is modified by providing an additional insulation layer of wood wool over the roof and wall. The air conditioning unit is located on the east facing wall at the height of 3 m from the floor. The 2-dimensional model of the test case room is created in the Gambit software through Cartesian coordinates and shown in Fig. 1. The traditional room is improvised through three modifications as mentioned in Table 1.

The model created in the Gambit software is meshed with the quadrilateral grid of size 0.01 m and imported to the FLUENT software for solving the computational domain. This grid structure is independent of the result as it is verified by repeating the test with a greater number of cells. The material properties of the building construction materials are given in Table 2.

2.1. Assumptions

(i) The heat conduction in the composite roof is one dimensional and the end effects are neglected.
(ii) The thermal conductivity of roof materials is considered as constant and not varying with respect to temperature.
(iii) Interfacial resistance is neglected.
(iv) The doors and windows are closed and the air leakage is neglected.
(v) East facing wall is the exterior wall, other is the interior wall
(vi) Adjacent rooms have no air conditioning unit.
(vii) The parametric values of air supply from the air conditioning unit are constant.

2.2. Governing equations of fluid flow and heat transfer

The fundamental equations that govern the fluid flow are conservation of mass, momentum and energy.

Conservation of Mass

$$\frac{\partial \rho}{\partial t} + \frac{\partial (\rho v_x)}{\partial x} + \frac{\partial (\rho v_y)}{\partial y} = 0 \tag{1}$$

Conservation of momentum

The momentum equation in the x direction is given in Eq. (2)

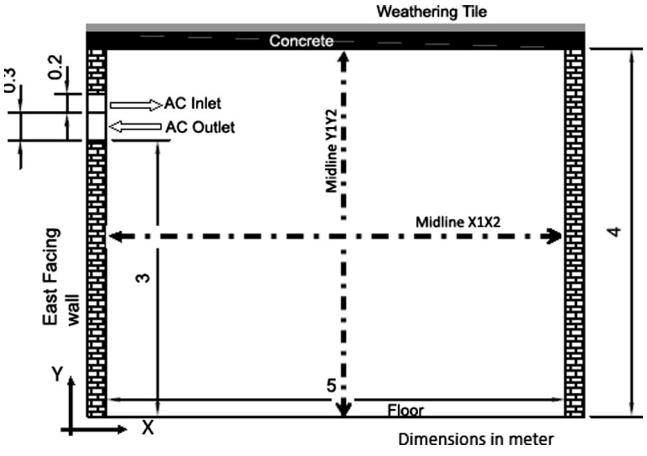

Figure 1 Computational model of test case room.

Table 1 Room with modified roof details.

Room case	Roof/wall modification
Room A	Traditional room: roof with concrete 0.15 m and Weathering tile 0.02 m
Room B	Wood wool layer is inserted between concrete and weathering tile with thickness of 0.02 m
Room C	Wood wool layer is inserted between concrete and weathering tile with thickness of 0.06 m
Room D	Additional wood wool layer of thickness 0.02 m is attached outside of the east facing wall of the room C

Table 2 Thermal properties building envelop material [19].

Roof material	Density (kg/m^3)	Thermal conductivity (W/mK)	Specific heat (J/kg K)
Concrete	2300	1.279	1130
Weathering tile	1300	0.25	1300
Wood wool	500	0.1	1000
Brick	1150	0.262	–

$$\frac{\partial \rho v_x}{\partial t}+\frac{\partial(\rho v_x v_x)}{\partial x}+\frac{\partial(\rho v_x v_y)}{\partial y}=\rho g_x-\frac{\partial P}{\partial x}+R_x+\frac{\partial}{\partial x}\left(\mu_e\frac{\partial v_x}{\partial v_x}\right)+\frac{\partial}{\partial y}\left(\mu_e\frac{\partial v_x}{\partial y}\right)+\tau_x \quad (2)$$

The momentum equation in the y direction is given in Eq. (3)

$$\frac{\partial \rho v_y}{\partial t}+\frac{\partial(\rho v_x v_y)}{\partial x}+\frac{\partial(\rho v_y v_y)}{\partial y}=\rho g_y-\frac{\partial P}{\partial y}+R_y+\frac{\partial}{\partial x}\left(\mu_e\frac{\partial v_y}{\partial v_x}\right)+\frac{\partial}{\partial y}\left(\mu_e\frac{\partial v_y}{\partial y}\right)+\tau_y \quad (3)$$

where v_x, v_y and v_z are the components of velocity in x, y and z directions, ρ is the density, t is the time, g is the gravity, μ_e is the effective viscosity, P is the pressure, R_i is the source term for distributed resistance, suffix i is x, y and z,τ is the viscous loss.

Conservation of energy

$$\frac{\partial}{\partial t}(\rho C_p T_o)+\frac{\partial}{\partial x}(\rho v_x C_p T_o)+\frac{\partial}{\partial y}(\rho v_y C_p T_o)=\frac{\partial}{\partial x}\left(K\frac{\partial T_o}{\partial x}\right)+\frac{\partial}{\partial y}\left(K\frac{\partial T_o}{\partial y}\right)+W^v+E_k+Q_v+\phi+\frac{\partial P}{\partial t} \quad (4)$$

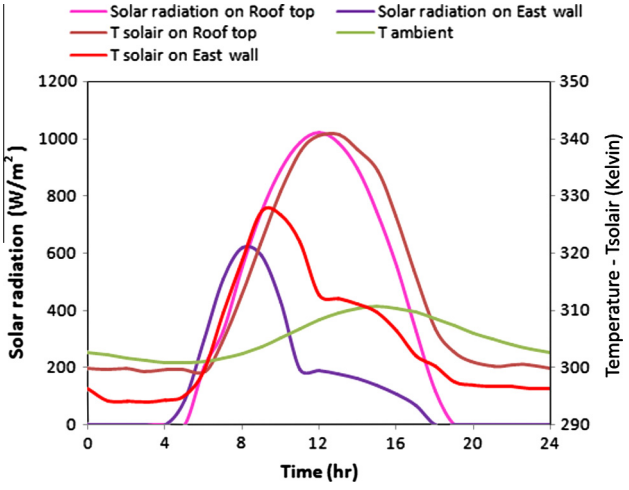

Figure 2 Solar radiation and solair temperature data for the month of may at Chennai.

where C_p is the uniform specific heat, T_o is the total temperature, K is the thermal conductivity, W^v is the viscous work term, Q_v is the volumetric heat source, ϕ is the viscous heat generation term and E_k is the kinetic energy.

Heat transfer across the roof and wall

$$\rho C_p\frac{\partial T}{\partial t}=\frac{\partial}{\partial x}\left(k\frac{\partial T}{\partial x}\right)+\frac{\partial}{\partial y}\left(k\frac{\partial T}{\partial y}\right)+\frac{\partial}{\partial z}\left(k\frac{\partial T}{\partial z}\right)+q-2h(T-T_\infty)-2\sigma\varepsilon(T^4-T_\infty^4) \quad (5)$$

where, ρ is the density, C_p is the specific heat, k is the thermal conductivity, q is the surface heat flux (power source) intensity,

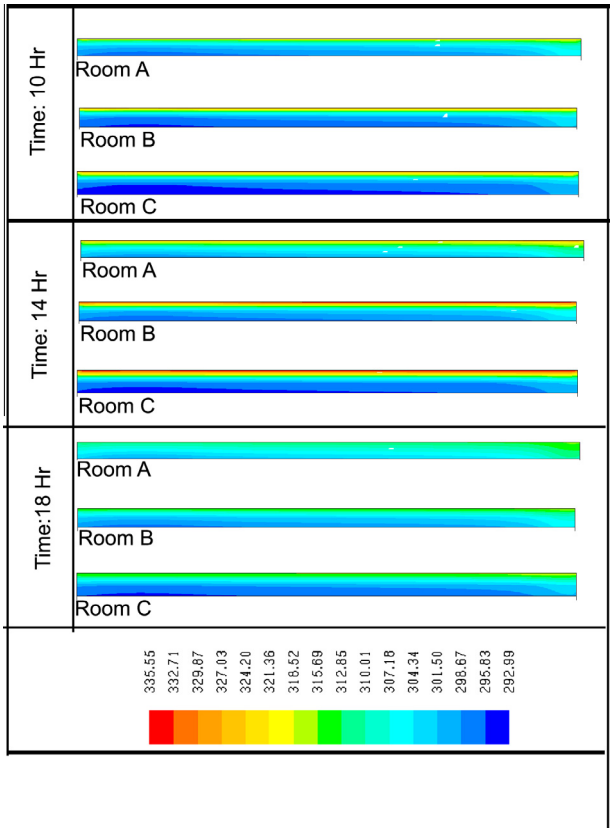

Figure 3 Temperature profile across roof with and without insulation.

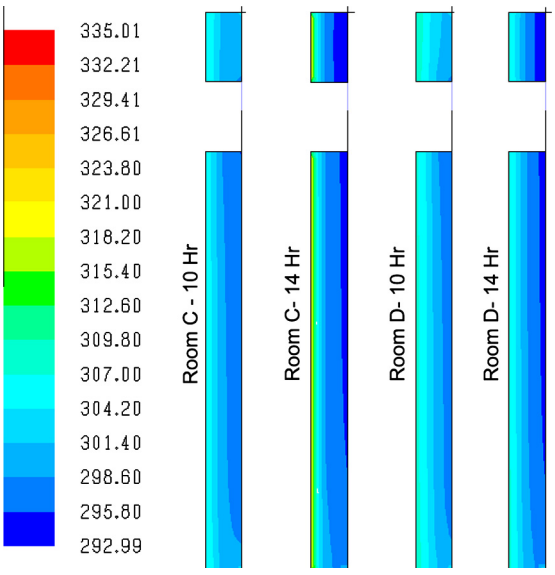

Figure 4 Temperature profile across exposed wall with and without insulation.

T is the temperature, t is the time, h is the convective heat transfer coefficient, σ is the Stefan–Boltzmann constant, ε is the emissivity of the surface, and T_∞ is the surrounding temperature.

2.3. Boundary conditions and solution methodology

The roof top surface and east facing wall are exposed to the solar radiation. Solar radiation data for the month of May at Chennai [20] are collected, converted into T_{solair} through the Eq. (1) and are shown in Fig. 2.

$$T_{\text{solair}} = T_a + (\alpha q / h_o) \tag{6}$$

where T_a is the ambient temperature, α, absorptivity, q, solar radiation and h_o convective heat transfer coefficient at the outer surface.

The supply air temperature of the air conditioned unit is specified as 293 K with a velocity of 3 m/s at an angle of 20° with respect to the floor taken in counter clockwise direction. The heat generation from human beings and electrical devices is assumed as 100w/m^2. K–ε turbulence model is employed to define the turbulence nature of flow. The turbulent intensity and length scale are defined as 4.4% and 0.1 m respectively. The room domain is initially analyzed under steady state with double precision segregated solver. Later it is solved under transient state for one complete cycle of 24 h with second order implicit method. All the cases are iterated up to the convergence level of 10^{-6}. The above numerical simulation is validated with the experimental predictions made by Pasupathy and Velraj [21]. In this validation, the same roof model made by Pasupathy and Velraj [21] is modelled in GAMBIT software and the same boundary conditions are

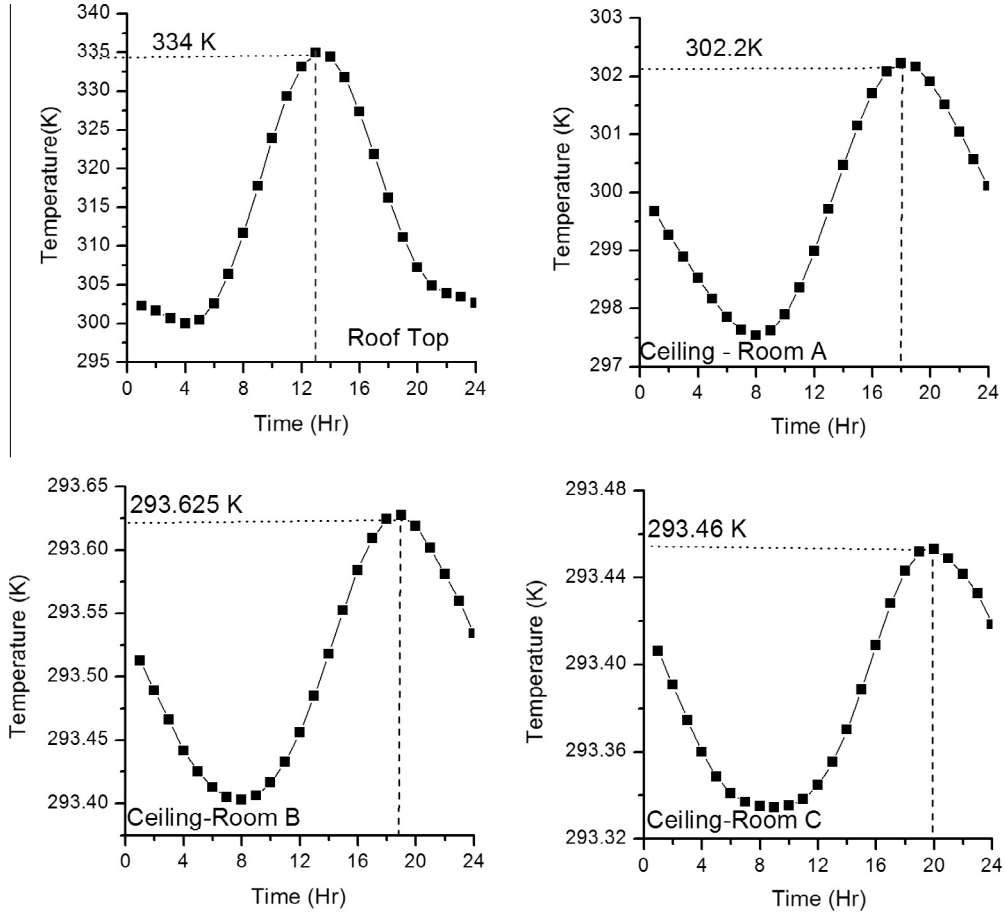

Figure 5 Average temperature at Roof top and ceiling for 24 h.

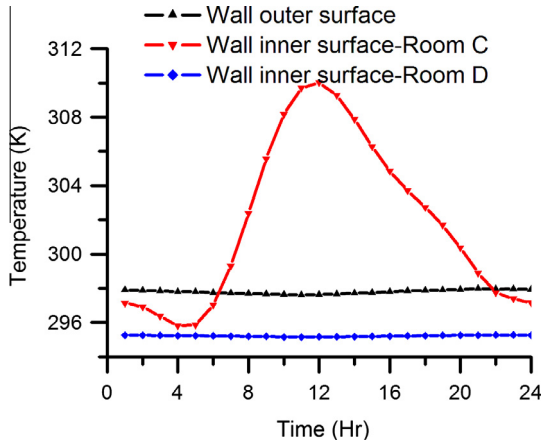

Figure 6 Average temperature of exposed wall outer and inner surface for 24 h.

applied. The numerically simulated temperature at the bottom of the roof surface is compared with the experimental predictions and validated [5,22].

3. Heat transfer across ceiling and wall

The temperature variation across the ceiling and wall for the insulated and non insulated room was predicted and shown in Fig. 3. In this figure, the temperature profiles across the roofs for the room A, B and C are shown for the time of 10 h, 14 h and 18 h. At time = 10 h, the temperature varies from roof top to ceiling as 314 K to 298 K for room A. For the rooms B and C the temperature variation is noticed as 322 K to 293.6 K and 323.9 K to 293 K respectively. Similarly the temperature variation at time = 14 h is noticed as 321 K to 300.5 K, 331 to 294 K and 334 K to 293 K for the rooms A, B and C respectively. At the 18th hr, the temperature varies from roof top to ceiling as 311.3 K to 302.2 K, 314 K to 294.6 K and 316 K to 293 K. Thus in the time range of 10–18 h the variation of ceiling temperature is almost negligible for room C and maintained constant as 293 K and comparatively lower than other rooms A and B. For the room case of B and C the roof temperature is noticed as comparatively higher than room A and this is due to the presence of insulation layer in Rooms B and C which strongly restricts the transfer of heat to the ceiling and hence leads to a local heating above the insulation layer. The temperature profile for the room with and without insulation along the east facing side wall is shown for the time of 10 h and 14 h in Fig. 4. For the room C the temperature variation from the outer surface of wall to inner surface is noticed as 307–298 K and for the wall with insulated material the variation is from 311 K to 293 K. This shows the presence of insulation material reduces the temperature of inner surface by 5 K. Additionally, the average temperature of the ceiling and roof top is also predicted for one complete 24 h for the rooms A, B and C and is shown in Fig. 5. The average temperature of roof top is almost constant up to 6 h and a drastic rise is noticed up to 13 h as 333 K and later falls down in the similar trend. For the room A, the average ceiling temperature falls down up to 8 h and the least temperature is noticed as 297.5 K. Later the temperature rises from 297.5 K to 302.2 K for the time of 18 h and again falls down. For the room B, the temperature falls from 293.5 K to 293.4 K up to the time of 8 h and raised to 293.62 K at 19th hr. For the room C, the ceiling temperature falls from 293.4 K to 293.3 K up to 7th hr and almost constant between 7 and 12 h and rises to a peak value of 293.46 K at the 20th hr. From this graph, it is inferred that the average temperature of the ceiling is almost constant for one complete 24 h for the room with insulation material and also the time of attaining the peak temperature is shifted from 17 h to 20 h for the room with out and with insulation material respectively.

Also the average temperature for the wall's outer and inner surface is predicted for the rooms C and D and shown in Fig. 6. The outer surface temperature almost constant up to 6 h and later rises significantly to a value of 310 K at 12th hr and after noon it gets linearly reduced. The wall's inner surface temperature is constant for the rooms C and D; however, the temperature is comparatively lower for room D by 3 K.

4. Indoor comfort of room with modified roof/wall

The average temperature along the midline X1 X2 and Y1Y2 is predicted for 24 h in rooms A, B, C and D and shown in Fig. 7.

Midline X1X2, Y1Y2 is positioned parallel to the floor and east facing wall at a distance of 2 m and 2.5 m respectively. For

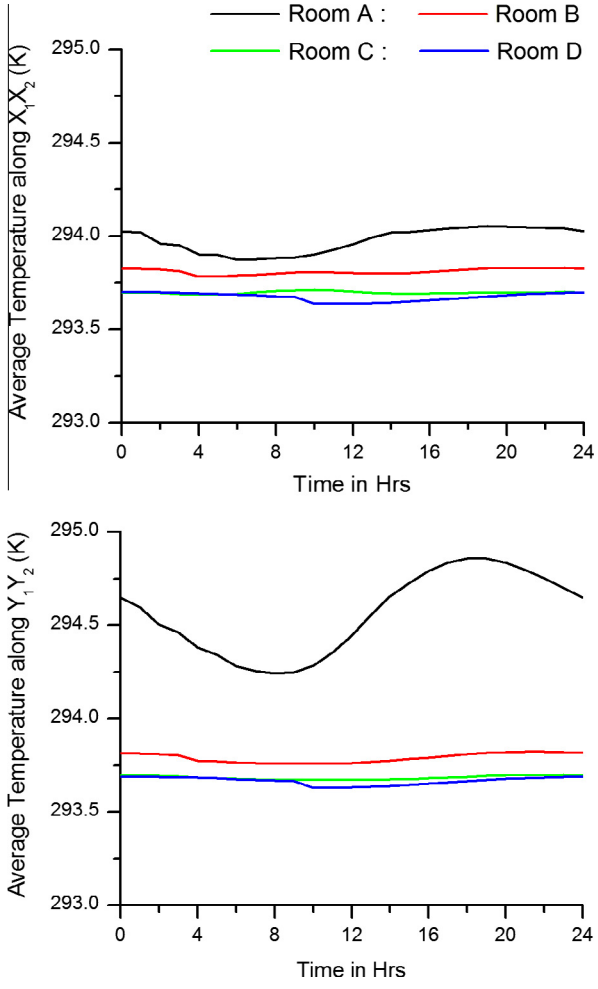

Figure 7 Average temperature variation along midlines for 24 h.

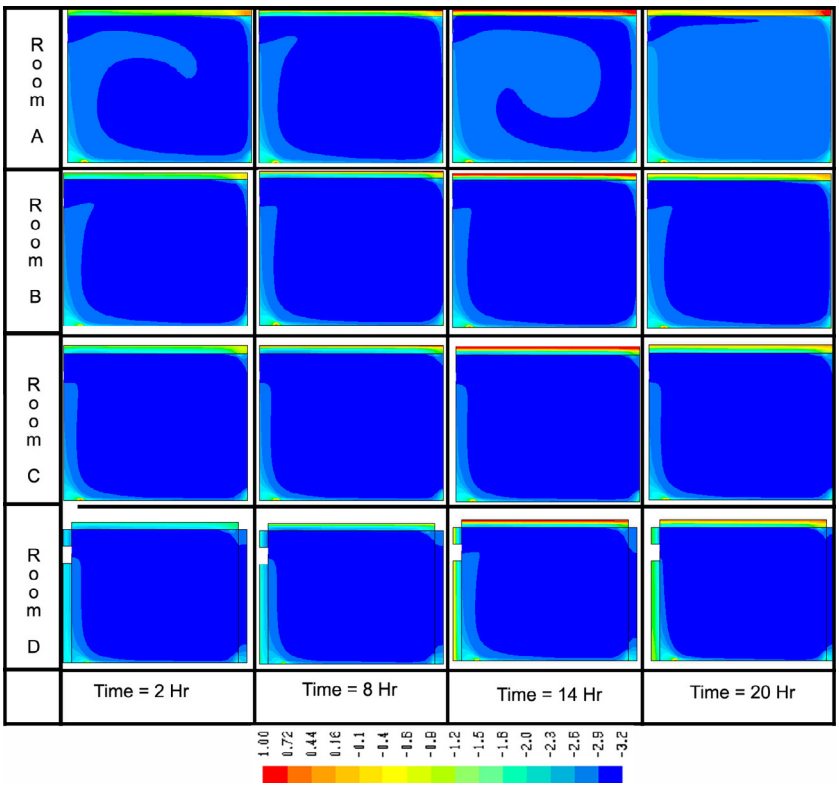

Figure 8 Predicted mean vote (PMV) contour for the rooms A, B, C and D for the time = 2, 8, 14 and 20 h.

the room A, the average temperature along X1X2 is about 294 K at time = 0 h and falls slightly up to 8th hr. From 8th hr to 14th hr the average temperature rises gradually to 294 K and from 14th hr to 24th hr it is almost constant. For room B, the average temperature along the midline X1X2 is almost constant at about 293.8 K and comparatively lesser than room A. In the room C, the average temperature is further reduced by 0.2 °C and maintained constant at 293.6 K. Rooms C and D show almost similar trend except between the time 6th and 17th hr. During this time room D shows comparatively lesser temperature than room C. The average temperature along the midline Y1Y2 shows a significant variation in room A. The average temperature falls from 294.6 K at time = 0 h to 294.25 K at 8th hr, after 8th hr the temperature rises linearly to 18th hr as 295.8 K and later falls gradually at the end of one cycle. However, other rooms B, C and D show almost constant temperature for a complete 24 h with a value of 293.79 K, 293.68 K and 293.66 K respectively.

Fig. 8 shows the predicted mean vote (PMV) contour for the rooms A, B, C and D at the time of 2nd, 8th, 14th and 20th hr. The PMV value is calculated from Fanger's thermal comfort equation [23,24] given in Eq. (7).

$$\begin{aligned} PMV = {} & (0.303e^{-0.036M} \\ & + 0.028)\{(M - W) - 3.05 \times 10^{-3}[5733 \\ & - 6.99(M - W) - p_a] - 0.42[(M - W) - 58.15] \\ & - 1.7 \times 10^{-5} M(5867 - p_a) - 0.0014M(34 - T_a) \\ & - 3.96 \times 10^{-8} f_{cl}[(T_{cl} + 273)^4 - (T_r + 273)^4] \\ & - f_{cl} h_c (T_{cl} - T_a)\} \end{aligned} \quad (7)$$

where M = Metabolic rate, W = Work done, pascal is the vapor pressure of the surrounding air, f_{cl} = factor of clothing, T_{cl} = clothing surface temperature, T_r = mean radiant temperature, hc = convective heat transfer coefficient. In the equation 2.28, the Metabolic rate = 70 W/m^2, work done = 30 W and thermal resistance of the clothing = 0.11(m^2 K)/W and relative humidity, RH = 50%.

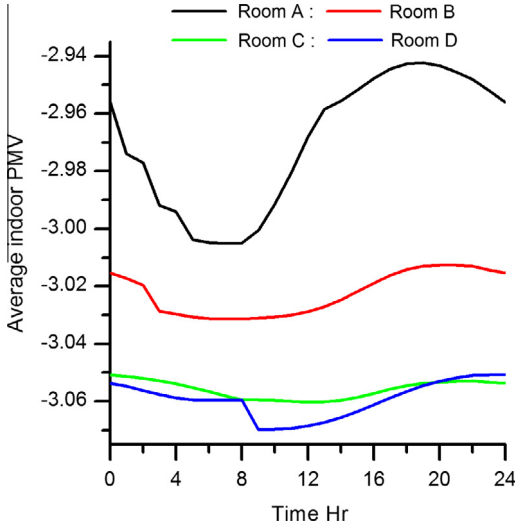

Figure 9 Average indoor PMV for the rooms A, B, C and D for 24 h.

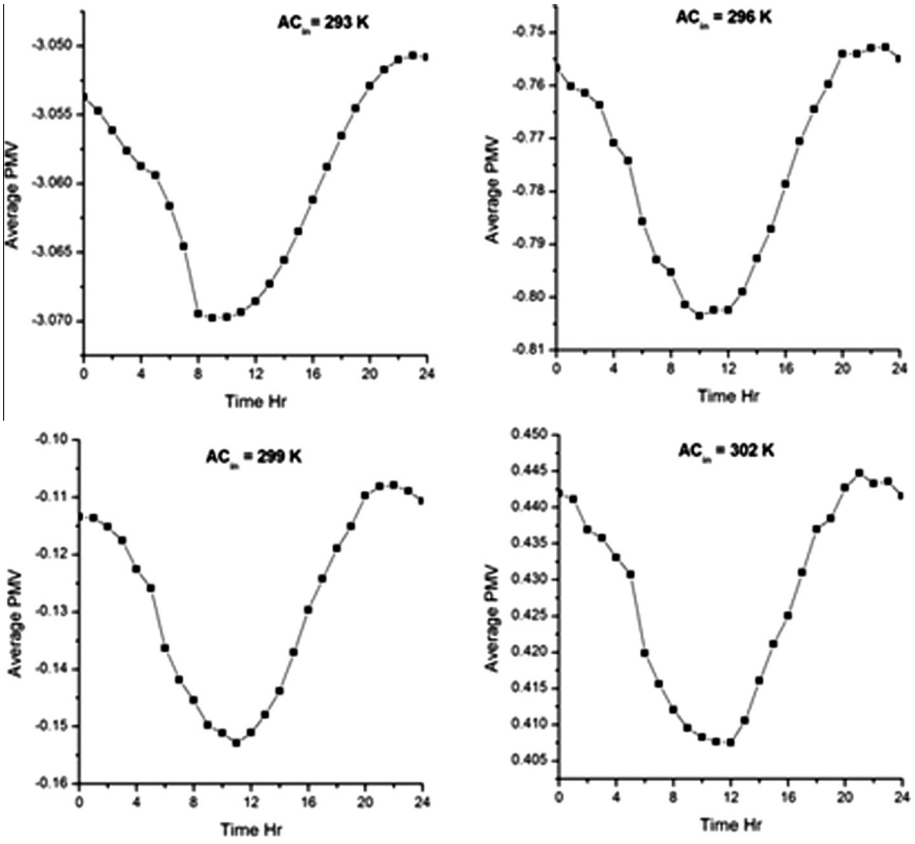

Figure 10 Average indoor PMV for AC_{in} value of 293–302 K.

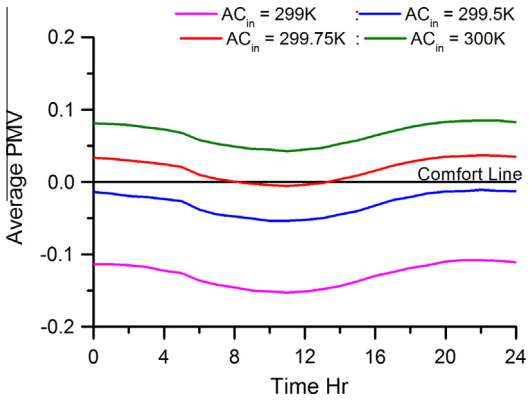

Figure 11 Average indoor PMV for fine adjusted AC_{in} value.

Temperature of the clothing (T_{cl}) was calculated from the Eq. (8) given below:

$$T_{cl} = 35.7 - 0.028(M - W) - 0.155I_{cl}\{3.96 \times 10^{-8} f_{cl}\left[(T_{cl}+273)^4 - (T_r+273)^4\right] + f_{cl}h_c(T_{cl} - T_a)\} \quad (8)$$

The convective heat transfer coefficient can be calculated from the Eq. (9).

$$h_c = 2.38(T_{cl} - T_a)^{0.25} \quad (9)$$

The mean radiant temperature (T_r) was computed from the average wall temperature, since there were no significant difference between wall temperatures.

$$T_r = \sum_{i=1}^{4} T_i F_{p-i} \quad (10)$$

where T_i is the temperature value at the ith wall and F_{p-i} is the radiation shape factor from face p of the gird cell to the visible surface i.

The PMV value has a range of +3.0 to −3.0, corresponding with the hot and cold thermal conditions. However in this study the PMV value reached beyond −3 which show that higher medium of indoor cooling. For the room A, at 2nd hr, few portions nearer to the floor and the east facing wall have a PMV of −2.9 and rest of the portions attains the PMV of −3.2. At the 8th hr, the entire room's interior except from small portion nearer to east facing wall has a PMV of −3.2. However at 14th hr, zones nearer to roof, west wall and floor have a PMV of −3.2 and rest of the portions are having −2.9. At 20th hr the entire indoor is having a PMV of −2.9 which shows that high solar radiation at the time of 14th hr makes comparatively less comfort up to the time of 20 h. For other rooms B, C and D the indoor PMV value almost similar and constant for all the time with a value of −3.2. This Fig. 5 is not enough to compare the comfort performance among the room with insulations and hence the average indoor PMV for a complete 24 h is predicted and shown in Fig. 9.

In Fig. 9, the average indoor PMV value of room A is −2.96 at time = 0 h and found reduced significantly to −3.0

at 8th hr and rises linearly to −2.95 at time = 18 h and later on falls slightly. Even though the air conditioner unit is supplying the air at constant temperature of 293 K the room indoor comfort is greatly affected by solar radiation. Also the maximum solar radiation value is attained at 14th hr and at later period the intensity of radiation gets reduced. However, the indoor PMV still gets raised up to a time of 20 h. This is due to the accumulation of solar radiation by the roof during the time period of 14–20 h. For the room B, the indoor PMV fluctuation is greatly reduced in comparison with room A and the average PMV value is almost constant at about −3.02. Further increase in the thickness of wood wool layer to 6 cm reduces the average indoor PMV by −0.03 and also provides uniform comfort. Room D shows reduced PMV value from the time of 0 h to 20th hr in comparison with room C. This reduction in PMV in insulated rooms is due to the restriction of heat transfer through east facing wall and roof by wood wool. From this study it is clearly noticed that providing the room insulations reduces the entry of solar radiation and hence the cooling energy produced by the air conditioning unit will be effectively utilized to keep indoor in a desired comfort level.

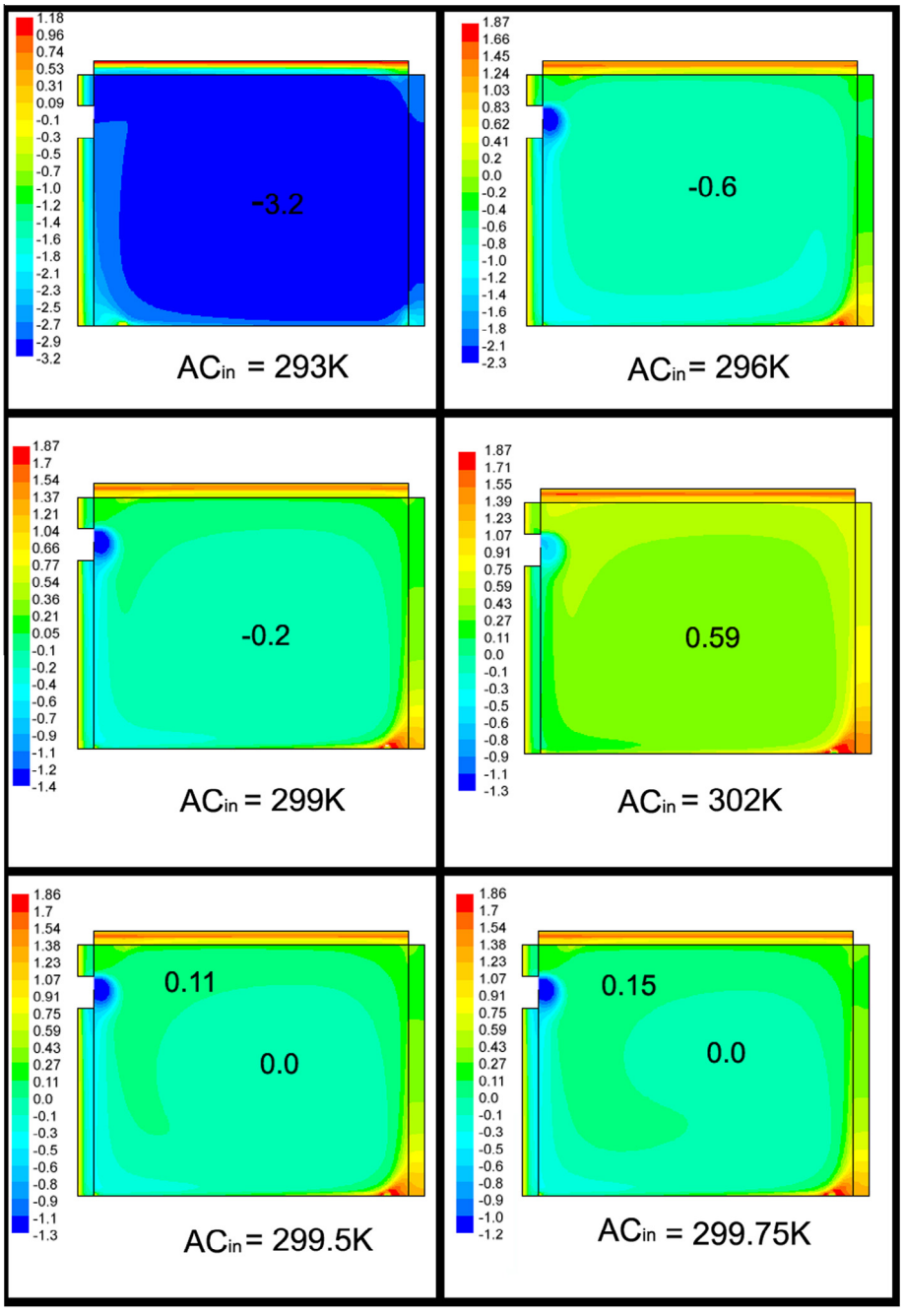

Figure 12 PMV contour plot for room D under various AC_{in} value.

5. Optimum setting of air conditioning unit for good thermal comfort

In the previous section the performance of room with different roof insulation patterns is discussed for the air conditioning unit supply temperature (AC_{in}) of 293 K. However this AC_{in} value cools the indoor adequately and causes negative discomfort. Hence in this section the optimum setting of air conditioning unit supply air temperature is identified to provide better comfort. Also, occupants are not having much awareness in setting the supply air temperature of air conditioning unit for a good thermal comfort and most frequently changing the operating temperature value to the extreme cool condition in a random fashion. Operating in such a condition causes various health problems and also consumes electrical energy in an undesirable way. Hence this study especially focused to identify the optimum level of air supply temperature of an air conditioning unit during the summer season. The air conditioning unit supply temperature is varied from 293 K to 302 K with an increment of 3° and the thermal comfort prevailed inside the room D is predicted and discussed.

The average indoor PMV value is predicted for one complete 24 h for different AC_{in} values and is shown in Fig. 10.

For all the values of AC_{in} the trend in the variation of average PMV is similar, that is the average PMV value gets decreased gradually from 0 to 11th hr, from 11 to 20th hr the average PMV value rises gradually and later on it is almost constant. The average PMV value changes from −3.055 to −3.07, −0.76 to −0.805, −0.11 to −0.14 and 0.445 to 0.410 for the AC_{in} value of 293, 296, 299 and 302 K respectively. The average PMV value changes negative to positive value for the AC_{in} change of 299 K to 302 K. Hence the AC_{in} value is fine adjusted from 299 K as 299.5, 299.75 K and 300 K and the average indoor PMV is predicted and shown in Fig. 11.

The average PMV value for the AC_{in} = 299.5 K is almost constant at about −0.74 and it is below the comfort line. However the average PMV for AC_{in} = 300 K follow above the comfort line with the value of 0.06 and for AC_{in} = 200.75 K travels very closer to the comfort line for one complete 24 h. The PMV contour plot for various AC_{in} value at 14th hr is shown in Fig. 12 which gives additional information regarding the comfort regions.

For AC_{in} = 293 K, the maximum portion of the room indoor has the PMV value of −3.2 and this value corresponds to extreme cold discomfort condition. Hence the AC_{in} value is raised to 296 K and in this condition, except the portions nearer to floor and east facing wall have the PMV of −0.6. However the remaining zones have the PMV of −0.4. For the case of AC_{in} = 299 K, the room interior up to a height of 3 m from the floor has the PMV of −0.2 and the portions nearer to the roof maintains the PMV of −0.1. Further increase in AC_{in} to a value of 302 K, the indoor PMV value shifted from cold condition to hot condition with a marginal value. For this AC_{in} value, the indoor PMV was maintained at 0.59 up to a height of 3 m from the floor and above that the PMV value is raised to 0.75. Since the PMV value shifted from negative to positive for the change of AC_{in} 299 K to 302 K, the AC_{in} value was further fine adjusted as 299.5 and 299.75 K. For these AC_{in} values, the major portions of the room indoor are maintained at the PMV value of 0.0 and this range of AC_{in} value is identified as the best setting of supply temperature for air conditioning unit for one complete 24 h.

6. Conclusion

The indoor thermal comfort of an air-conditioned room with roof and wall insulations is analyzed using CFD technique. The wood wool material is used as insulation layer which is identified as a cost effective and easily available material. Four types of building room are investigated namely traditional room (roof made of concrete and weathering tile- room A), room with additional insulation layer wood of 2 cm thick between concrete and weathering tile (room B), same room with wood thickness of 6 cm (room C) and room with wood wool on both roof and wall (room D). All the room cases are analyzed for the summer season, simulated under transient approach for a complete 24 h and validated experimentally. As an outcome of this analysis, the indoor predicted mean vote value and the temperature variation across the roof and wall are predicted at various time intervals. From this study, it is identified that the average indoor predicted mean vote for room D is comparative lesser as −3.05 for the given air conditioner supply air temperature of 293 K. However for the same condition, room A yields an average PMV of – 2.9. Also, the temperature at ceiling and exposed wall inner surface is reduced by 6.8 K and 3 K respectively for insulated room in comparison with noninsulated room. From this, it is clearly identified that insulated room restricts the heat gain due to solar radiation and hence the cool energy possessed by the supply air is effectively utilized to cool the indoor. However, for the supply air temperature of 293 K, the average PMV value is −3.05 which pertains to the condition of extreme cool discomfort. Hence an optimum setting of supply air temperature is identified by analyzing the same room D under various AC_{in} value and predicted as in the range of 299–300 K. This optimum setting of AC_{in} value for an insulated building room helps the occupants to live in thermally comfortable environment with comparatively less consumption of cost for energy.

References

[1] Jim CY. Air-conditioning energy consumption due to green roofs with different building thermal insulation. Appl Energy 2014;128:49–59.
[2] Sookchaiya Thammanoon, Monyakul Veerapol, Thepa Sirichai. Assessment of the thermal environment effects on human comfort and health for the development of novel air conditioning system in tropical regions. Energy Build 2010;42(10):1692–702.
[3] Vijaykumar KCK, Srinivasan PSS, Dhandapani SA. Performance of hollow clay tile (HCT) laid reinforced cement concrete (RCC) roof for tropical summer climates. Energy build 2007;39(8): 886–92.
[4] Chou Huann-Ming, Chen Chang-Ren, Nguyen Vu-Lan. A new design of metal-sheet cool roof using PCM. Energy Build 2013;57:42–50.
[5] Prakash D, Ravikumar P. Transient analysis of heat transfer across the residential building roof with pcm and wood wool-a case study by numerical simulation approach. Arch Civil Eng 2013;59(4):483–97.
[6] Barrios G, Huelsz G, Rechtman R, Rojas J. Wall/roof thermal performance differences between air-conditioned and non air-conditioned rooms. Energy Build 2011;43(1):219–23.

[7] Vijayalakshmi MM, Natarajan E, Shanmugasundaram V. Thermal behaviour of building wall elements. J Appl Sci 2006;6:3128–33.
[8] Ozel M, Optimum Pihtili K. location and distribution of insulation layers on building walls with various orientations. Build Environ 2007;42(8):3051–9.
[9] Al-Sanea SA, Zedan MF, Al-Hussain SN. Effect of thermal mass on performance of insulated building walls and the concept of energy savings potential. Appl Energy 2012;89(1):430–42.
[10] Aye Lu WW, Charters S, Fandiño AM, Robinson JRW. Thermal Performance of Sustainable Energy Features; 2005.
[11] Al-Sanea SA, Zedan MF. Effect of insulation location on thermal performance of building walls under steady periodic conditions. Int J Ambient Energy 2001;22(2):59–72.
[12] Halwatura RU, Jayasinghe MTR. Thermal performance of insulated roof slabs in tropical climates. Energy Build 2008;40(7):1153–60.
[13] Alvarado LJorge, Terrell Jr Wilson, Johnson Michael D. Passive cooling systems for cement-based roofs. Build Environ 2009;44(9):1869–75.
[14] Kumar Ashok, Sumar BM. Experimental evaluation of insulation materials for walls and roofs and their impact on indoor thermal comfort under composite climate. Build Environ 2013;59:635–43.
[15] FLUENT news, Spring; 2001.
[16] Stamou AI, Katsiris Ioannis, Schaelin Alois. Evaluation of thermal comfort in Galatsi Arena of the Olympics Athens 2004 using a CFD model. Appl Therm Eng 2008;28(10):1206–15.
[17] Fan CY. Air conditioning design and engineering practice of large space buildings. Beijing: China Architecture and Building Press; 2001.
[18] Bin By Zhao, Ying Li, Xianting Li, Qisen Yan. Numerical analysis and improvement of air flow pattern for the Great Hall of the People. Build Energy Environ 2000;04.
[19] Kothandaraman CP, Subramanyan S. Heat and mass transfer data book. New Delhi, India: New age international publisher; 2004.
[20] Tiwari GN. Solar energy of fundamentals, design, modeling and applications. New Delhi: Handbook of Narosa publishing house; 2001.
[21] Pasupathy A, Velraj R. Effect of double layer phase change material in building roof for year round thermal management. Energy Build 2008;40(3):193–203.
[22] Prakash D, Ravikumar P. Multi-objective optimization of residential building roof layer thickness for minimization of heat entering the room using FEM and grey relational analysis. J Inst Eng (India): Ser A 2014;95(1):1–9.
[23] Paramasivam Ravikumar, Prakash D. Analysis of thermal comfort in an office room by varying the dimensions of the windows on adjacent walls using CFD: a case study based on numerical simulation. Build Simulat 2009;2(3):187–96.
[24] Awbi HB. Ventilation of buildings. 2nd ed. New York: Spon Press; 2003.

D. Prakash, completed his BE-Mechanical engineering in Bharathidasan University and ME-Engineering design at Bharathiyar University. He joined as a part time research scholar at Anna University in the year 2007. In his academic career, he published 9 journals and 15 papers at conference.